Geomechanics and Engineering, *Vol. 20, No. 2 (2020) 113-120*
DOI: https://doi.org/10.12989/gae.2020.20.2.113

Experimental investigation on multi-parameter classification predicting degradation model for rock failure using Bayesian method

Chunlai Wang*[1], Changfeng Li[1], Zeng Chen[1], Zefeng Liao[1], Guangming Zhao[2], Feng Shi[1] and Weijian Yu[3]

[1]School of Energy and Mining Engineering, China University of Mining and Technology Beijing, 100083, Beijing, China
[2]School of Energy and Safety Engineering, Anhui University of Science and Technology, 232001, Huainan, Anhui, China
[3]School of Resource and Environment and Safety Engineering, Hunan University of Science and Technology, 411201, Hunan Xiangtan, China

(Received February 11, 2019, Revised October 25, 2019, Accepted January 4, 2020)

Abstract. Rock damage is the main cause of accidents in underground engineering. It is difficult to predict rock damage accurately by using only one parameter. In this study, a rock failure prediction model was established by using stress, energy, and damage. The prediction level was divided into three levels according to the ratio of the damage threshold stress to the peak stress. A classification predicting model was established, including the stress, energy, damage and AE impact rate using Bayesian method. Results show that the model is good practicability and effectiveness in predicting the degree of rock failure. On the basis of this, a multi-parameter classification predicting deterioration model of rock failure was established. The results provide a new idea for classifying and predicting rockburst.

Keywords: rock failure; multi-parameter; acoustic emission; Bayesian; classified predicting

1. Introduction

Rock failure is more complex under the external load; it is difficult to predict rock failure accurately (Cook 1992, Brady 1969). The excavated roadway destroys the mechanical balance around the rock mass in the working face, resulting in the brittle failure and energy release, and rock bursts are prone to happen (Konicek and Waclawik 2018). Rockburst may cause the support equipment damage, casualties, collapse of the roadway, it affects normal mine safety seriously. Therefore, the prediction of rock failure is significant. During the rock rupture process, the shape changes, cracks occur, acoustic emission occurs, and even temperature and conductivity change. These are all precursors to rock failure. How to use this precursor information to conduct rock failure predicting has become a hot and difficult point in this field.

The phenomenon that rocks release elastic waves during the process of destruction is called acoustic emission. Acoustic emission is an important precursor for predicting rockburst, which is valued by many researchers (Wang *et al.* 2018, 2013, Zhang *et al.* 2018). Many experts have made great work in rock fracture and prediction (Frid 2000, 2001, Goufo 2018, Vacek 2008, Wei *et al.* 2017, Zhao *et al.* 2008). In the failure process of brittle materials, acoustic emission (AE) monitoring technology is widely applied because of its real-time and dynamic monitoring of the generation and development of internal cracks (Watanabe 2001, Lockner 1993). Zhang (2018) used acoustic emission technology for monitoring, which has achieved the role of comprehensive monitoring on the spot. Wang (2018) found the relative quiet period of acoustic emission parameters, and used it as the precursor information of rock failure. Carpinteri *et al.* (2006) found the accelerated release of AE energy before the material was damaged. Stanchits *et al.* (2006) studied the effect of volume strain on AE velocity and found predicting information based on velocity. Wasantha *et al.* (2014) studied the energy release of dry sandstone under uniaxial compression using acoustic emission techniques. They found that there was a large amount of energy dissipated before the sample was eventually destroyed. Carpinteri *et al.* (2010, 2013, 2016) A bending test was performed and the results showed that the AE parameters would vary with product damage.

The simple use of AE signals could not provide a good predicting of rockburst, and other factors such as noise can seriously affect the accuracy of the calculation. The AE signal must be converted to establish a rockburst predicting model to achieve the purpose of predicting. Therefore, many researchers have conducted research in this direction. Zhang *et al*. (1991) proposed the neural network methods, which could not only simulate the elastic behavior of materials, but also simulate elastoplasticity and plastic deformation to destroy materials. Zhu *et al*. (2008) established an improved support vector machine algorithm for rockburst prediction using many parameters such as maximum tangential stress, rock uniaxial compression, tensile strength and elastic energy index. Wang *et al*. (2015) established a multi-index model to predict rockburst, based on fuzzy matter-element theory, information entropy theory and closeness rules. Kang *et al*. (2017) proposed a novel fractional power model for wavelet packet transform analysis, which is used to decompose, filter and reconstruct

*Corresponding author, Professor
E-mail: tswcl@126.com

http://www.techno-press.org/?journal=gae&subpage=7
ISSN: 2005-307X (Print), 2092-6219 (Online)

AE signals, which improves the accuracy of positioning. Wang *et al*. (2013) used the Burgers model to study the position of the acoustic emission source in the granite sample under the uniaxial compression. The results show that the Burgers model can predict the rock failure mode under uniaxial loading conditions. However, these methods need be improved for the better results. Such as the neural network has the disadvantage of slow convergence rate; the Projection the selection of kernel function and parameters of V-SVR algorithm has certain randomness and has a great influence on the result; the fuzzy matter–element model method needs to give different weight to each index. The results used those theories are quite different, and they do not make different grades of predicting based on the degree of damage.

Bayesian method could be used to analyze the multivariate and quantificational problem (Agletdinov *et al.* 2016, Li *et al.* 2017, Wang *et al.* 2018) introduced a new Bayesian multi-index model to predict and evaluate rock bursts, which was observed to predict rock bursts more effectively than the current methods. Therefore, we carried out the AE experiment. Various precursory information of rock failure was analyzed, a comprehensive discriminant model was established based on Bayesian method to realize multi-parameter predicting. In addition, a deterioration model was built to analyze the degree of rock damage. A predicting grade classifier was established ultimately; it proposes a new method for the graded predicting rock failure in the field.

2. Experimental materials and methods

2.1 Experimental specimen and equipment

Rock samples were got from the roof of Xiezhuang deep mine in Shandong Province, China. Rock samples were cylindrical cores with diameter of 50 mm and length of 100 mm. The two end planes of every specimen were parallel within an accuracy of ± 0.05 mm, and both planes were perpendicular to the longitudinal axis with an accuracy of ± 0.25°. Specimens' basic physi-mechanical parameters were as shown in Table 1.

These specimens were loaded by a microcomputer-controlled electrohydraulic servo stiffness compressor (GAW-2000, Chaoyang Test Instrument CO., LTD, Changchun, China). AE monitoring system equipment includes the PCI-2 fully digital AE signal collection and the analysis system of Physical Acoustics Company (PAC CO., New Jersey, U.S.A.), as shown in Fig. 1(b).

2.2 Experimental methods

Six sensors were placed on the specimens according to the Fig. 1(a). Between the sensors and the surface of the rock, a proper amount of coupling agent was applied to contact fully, and it is assisted by adhesive tape. These sensors were arranged at the 20 mm at both ends of the specimen in order to reduce the end effect. AE monitoring system threshold was set to 45 dB according to the laboratory machine and environmental noise, and the sampling frequency was 1 MHz, and the gain of preamplifier was set to 40 dB. In addition, strain gauges are attached for measuring strain.

Table 1 Limestone basic physi-mechanical parameters

NO.	Length (mm)	Diameter (mm)	Density ($g \cdot cm^{-3}$)	*UCS (MPa)	Total ringing number
X_1	102.12	51.2	2.85	102.13	37182
X_2	99.42	48.7	2.68	97.7	43122
X_3	98.54	49.52	2.61	48.63	275298
X_4	97.84	48.3	2.64	55.26	42500
X_5	98.02	49.22	2.66	118.15	93710
X_6	101.2	50.5	2.71	124	43938
X_7	99.28	48.64	2.66	124	49463
X_8	98.4	51.6	2.67	97.72	41182

*The uniaxial compressive strength (UCS)

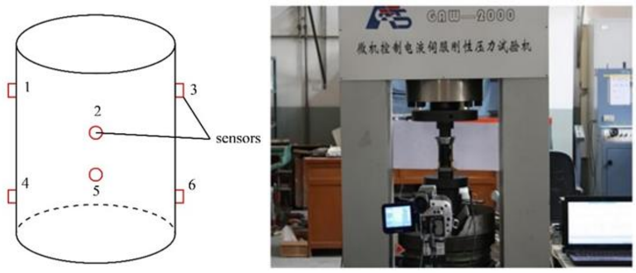

(a) (b)

Fig. 1 The arrangement of AE sensors and rock mechanics testing system

The experiment used the axial displacement loading control mode, and the loading rate was 0.005 mm/s. AE monitoring system and the loading system were always real time synchronized, the former collected the activity of AE during the loading, and the latter collected the process of mechanical parameters during loading.

3. Theoretical basis

3.1 Theoretical basis of Bayesian

Bayesian discriminant analysis is a statistical analysis method used to discriminate the type of sample. The basic idea is to calculate the prior probability and covariance of each classification under the premise of classifying the known observation samples, and establish a classification discriminant function for classification and discrimination, and then perform posterior probability calculation and back generation. Verify and determine which type of statistical analysis method the new sample belongs to. The main processes of modeling and calculation are as follows:

(1) Prior distribution

There are n observation samples, which are divided into k classifications, G_1, G_2, … G_k, obey the m-dimensional normal population distribution; n_i is the number of samples; and $X_j^{(i)} = [(x_1, x_2, \dots x_m)_j^{(i)}]^T$ is the observation matrix of the sample, $X_j^{(i)} \in G_i$, i=1,2,3, … k, j=1,2,3, … n_i.

Priori probability:

$$p_i = \frac{n_i}{n_1 + n_2 +, \ldots, n_k} = \frac{n_i}{\sum_{i=1}^{k} n_i} \tag{1}$$

n_i is the number of samples classified in the i-th category.

(2) Sample mean and covariance

Since G_i obeys the m-dimensional normal population distribution, the overall distribution characteristics of the i-th classification can be estimated by the sample mean and the sample covariance.

$$\mu X^{(i)} = \frac{1}{n_i} \sum_{j=1}^{n_i} X_j^{(i)} \tag{2}$$

$$S_i^2 = \frac{1}{n_i - 1} \sum_{j=1}^{n_i} (X_j^{(i)} - \bar{X}^{(i)})(X_j^{(i)} - \bar{X}^{(i)})^T \tag{3}$$

$$\sum = \frac{1}{\sum_{i=1}^{k}(n_i - 1)} \sum_{i=1}^{k} (n_i - 1) S_i^2 \tag{4}$$

where S_i^2 is the variance matrix of the samples of the i-th group; Σ is the covariance matrix of the samples.

(3) Establish a discriminant function

$$\omega_i(X) = \mu_i^T \Sigma^{-1} X - \frac{1}{2} \mu_i^T \Sigma^{-1} \mu_i + \ln p_i \tag{5}$$

p_i is the prior probability of G_i; μ_i is the mean matrix of the i-th sample; and Σ is the population covariance matrix of the sample. $X = (x_1, x_2, \ldots x_m)^T$ is the observed value of the sample, i=1,2,3, ... k.

The discriminating rule is: For X, if $\omega_i(X) = \max_{1 \le j \le k} \omega_j(X)$, then $X \in G_i$.

(4) Posterior probability and back verification

The generalized squared distance function of sample X to the i-th group is defined as $d_j^2(X)$:

$$d_j^2(X) = (X - \mu_j)^T \Sigma^{-1} (X - \mu_j) - 2 \ln p_j$$

Then X is to the posterior probability of the i-th group:

$$P(G_j|X) = \frac{\exp[-\frac{1}{2} d_j^2(X)]}{\sum_{i=1}^{k} \exp[-\frac{1}{2} d_i^2(X)]} \tag{6}$$

3.2 Discriminant and parameters of Bayesian

Bayesian discriminant is to calculate the prior probability and covariance of each classification based on the assumption of the specimens' classification, and the established the classification and discriminant function was classified. Bayesian discriminant can determine specimens belong to own classification. The parameters should be selected for the final more accurately prediction results. They are as follows:

(1) Damage stress threshold σ_d

The process of rock failure was accompanied by the closure, initiation, propagation and interaction of cracks. The mechanical properties of rock were related to the development of microcracks closely (Martin 1993, Eberhardt 1998). When the stress was over σ_d, the increased stress caused the cracks interpenetrate and form a macroscopic failure. Therefore, σ_d was scheduled as one of the discriminant parameters.

(2) Elastic energy W_{et}

Rock failure was a process of energy dissipation. It was sudden and violent release of elastic strain energy in rock (Li, 2018). Cook *et al.* (1966) proposed the rock burst energy index based on the theory of conservation of energy and answered questions about the source of rock burst. The stored elastic energy in the rock was closely related to the degree of the damage. The proposed elastic energy should be used as an index to predict rock burst. Therefore, the elastic energy W_{et} was selected as one of the discriminant parameters (Wang and Park 2001).

(3) Damage value D

Damage theory can describe the nonlinear dynamic process of rock fracture dynamically (Sato *et al.* 1986). Rock failure is actually the expansion of damage. The defined damage by AE parameters can indirectly represent the internal defects of rocks. The way of the damage value defined by AE parameters reference (Geng *et al.* 2017).

(4) AE impact parameters

The characteristics of rock failure could be expressed by AE impact parameters better than AE event. Therefore, the impact parameters were used to analyze the rock failure process. The model parameters, including in the Damage stress threshold σ_d, Elastic energy W_{et}, Damage value D, AE impact, were proposed to describe the internal damage and external characterization of rock fracture, it is more objective and accurate.

3.3 Deterioration model and predicting classification

Quantifying the degree of damage is the precondition for predicting classification. In this study, rock deterioration model L was constructed by the ratio of the peak stress to the predicting stress and breaking time. Making the two parameters into a unified scale, the normalization process was performed. The size of the numerical values was constant relative distance. For the specimen value range [x_{min}, x_{max}], the linear normalized function expression is:

$$y = \frac{x - x_{min}}{x_{max} - x_{min}} \tag{7}$$

where x, y are the converted values.

For stress σ, the range is [0, σ_c] and σ_c is the peak stress. The normalized expression as follows:

$$\sigma = \frac{x}{\sigma_c} \tag{8}$$

In order to reveal the degree of rock damage, the greater the σ_d, the more serious the rock is damaged, where x=σ_d.

For time T, the range is [0, T_c] and T_c is the time of rock fracture. The normalized expression as follows:

$$T = \frac{x}{T_c} \tag{9}$$

To indicate the length of the failure time, the x took the

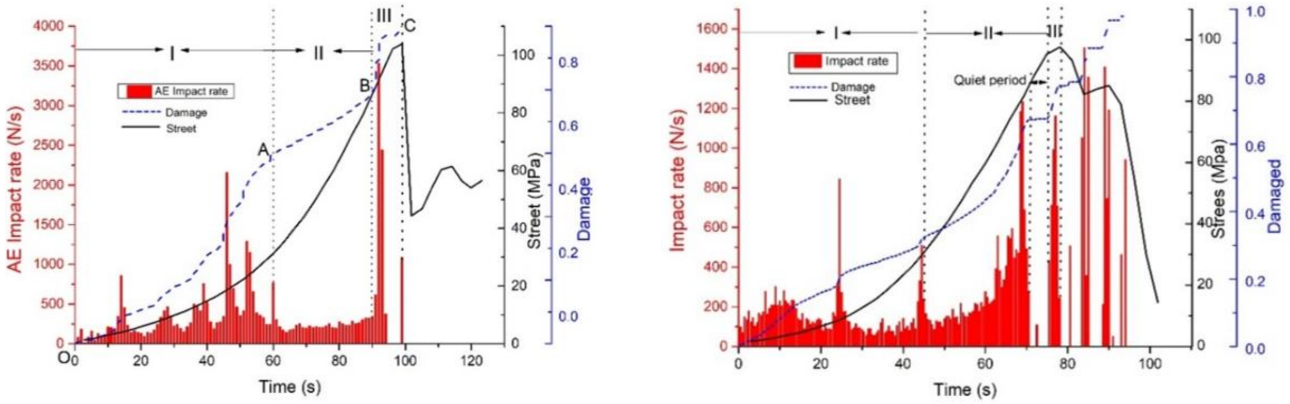

(a) (b)

Fig. 2 Relationship between street-time curve, AE impact rate, damage value for X_1 X_2

time interval between the predicting time and the time of failure, $x = T_c - T_d$. Because the degree of rock damage is positively related to Eq. (8) and negatively related to Eq. (9), the deterioration model was defined as follows:

$$L = \frac{\sigma}{T} = \frac{\sigma_d T_c}{\sigma_c (T_c - T_d)} \tag{10}$$

σ_d is the crack damage threshold, σ_c is the peak stress, T_d is predicting point, and T_c is the time of rock failure.

L is a dimensionless value, the greater the value, the more serious the rock damage, the closer to the peak stress, and the shorter the break time.

The $\frac{\sigma_d}{\sigma_c}$ ratio is used to indicate the predicting grades based on the L. The yield point was found generally about 75 percent the peak stress for brittle rocks. Therefore, the 75 - 80 percent peak stress can be defined as a third grade warning, and 80 - 85 percent is defined as a second grade warning, and 85 - 90 percent is defined as a first grade warning. Bayesian method is based on normal distribution.

4. Results and analysis

The curves of the stress, AE impact rate, damage value and time are shown in Fig. 2. X_1, X_2 are as examples.

4.1 The cracks fracture damage threshold

The impact rate corresponded to the activity of stress curve as shown in Fig. 2. When the stress was up to the peak stress, the amplitude and frequency of impact rate were much larger; there were several suddenly increase points. Cracks were up to the stage of mutual expansion, and cracks were expanding rapidly, rock was failure soon. Therefore, stress thresholds could be determined by AE activity characteristics at various stages of cracks propagation. X_1 and X_2 showed significant differences after stress peak. For the X_1, stress reached at the peak value, then the curve was vertical descending approximately, AE activity was disappeared, the damage value was the maximum, which indicated that the X_1 was completely failure and extremely brittleness. For the X_2, AE activity

Table 2 The cracks damage threshold

NO.	X_1	X_2	X_3	X_4	X_5	X_6	X_7	X_8
σ_d/(MPa)	89.64	80.72	38.37	42.26	99.49	107.3	103.7	57.02
$\frac{\sigma_d}{\sigma_c}$ (%)	87.78	82.62	78.9	76.48	84.21	86.53	86.53	86.54
D	0.79	0.60	0.48	0.56	0.65	0.72	0.85	0.72
R	3258	1230	2053	3258	1480	1280	1270	5702

still existed after the stress reached the peak stress, and the damage curve continued to increase, which indicated that the X_2 was not failure completely, the X_2 still had certain carrying capacity.

There were several saltation points in the cracks propagation stage; we defined the stress corresponding to the last saltation point as crack fracture damage threshold. Before this saltation point, rocks did not failure in large scale. At the saltation point, the damage value raised sharply, indicating that there was a large crack in the rock and the fracture surface was coalescent. Specimens' cracks damage threshold σ_d was defined, as shown in Table 2.

4.2 The evolution pattern of damage value D

The damage factor D of the coal sample obeys the statistical distribution, and its formula is as follows:

$$\varphi(F) = \frac{m}{F_0}(\frac{F}{F_0})^{m-1} exp[-(\frac{F}{F_0})^m]$$

The relationship between the damage factor D and the probability density of micro-destruction is:

$$\frac{dD}{dF} = \varphi(F)$$

Therefore:

$$D = \int_0^F \varphi(F) dF = 1 - exp[-(\frac{F}{F_0})^m]$$

When the sample is all destruction, the total acoustic emission is Ω_m. The cumulative acoustic emission during the destruction Ω can be expressed as:

$$\Omega = \Omega_m \int_0^F \varphi(x) dx$$

When $\varphi(x) = \varphi(F)$

$$D = \frac{\Omega}{\Omega_m} = 1 - exp[-\left(\frac{F}{F_0}\right)^m]$$

In this study, the damage was defined by the AE count. In the Fig. 2, the tendency of the damage curve had a good consistency with the AE impact rate. It showed the rationality of using AE parameters to define the rock damage value, and the damage value could show the damage evolution of the cracks. In addition, X_2 damage curve was saltation increasing phenomenon, and the periodicity of curve was obvious, this might be caused by more original cracks in the X_2 than X_1, these cracks were closed and the ringing counts suddenly increase.

This paper focused on the changes of damage value at the critical failure. The curve raised sharply (B point on the Fig.2 (a)), the tangent increased closing to positive infinity. This indicated the cracks were rapidly expanding and cut-through. The sample was going to fail. Therefore, the damage value at the sharp point was defined as the damage predicting value. The damage warning values D of the specimens were shown in Table 2.

4.3 The evolution pattern of AE impact rate R

The AE impact rate R is the number of impacts per unit time. This parameter is calculated by the supporting software of the acoustic emission experimental equipment. AE impact rate could describe the development, expansion and penetration of cracks in the rock specimens. As shown in the Fig. 2, AE characteristics could be divided into three stages, as I, II, and III. Which were corresponding to the stage of deformation and destruction of the rock. In I, the micro fissure was closed, AE activity was obvious, and the impact rate increased obviously with the loading. AE impact rate of X_2 specimen was obvious during I, which was due to the more internal original joints. However, the overall value of X_1 was larger than X_2, because X_1 was better integrity. More energy was stored in the loading process. In II, AE was relatively quiet, and the impact rate was in lower level. In III, when the loading status of rock sample was up to the plastic deformation stage, AE activity was active and the impact rate increased obviously. As shown in the Fig.2, there was a period of AE disappearing before rock failure for X_2, AE appeared the relatively quiet period. The specimen released a large amount of energy, and the impact rate of AE increased suddenly approach the failure, these phenomena could be as precursory information of rock failure. As show in Fig.2, when the impact rate of AE was up to the maximum, the stress was the peak. The maximum impact rate of AE could be defined as the predicting value of the rock failure. The maximum impact rate values of specimens were as follows, as shown in Table 2.

4.4 Deterioration value and multi-parameter predicting model

When the other conditions are the same, the more the rock receives the load, the easier it is to destroy. For rocks with low brittleness, the yield limit is generally about 75% of the peak load. Dividing early warning into different categories is the basis for grading early warning. Therefore, the value of sigma_*d* / sigma_*c* is 75%-80% can be set as a three-level warning, 80%-85% as a second-level warning, and 85%-90% as a first-level warning. Each predicting value was obtained, and the elastic energy stored at the moment of damage threshold was calculated. The results of the predicting grade for each specimen were as follows according to $\frac{\sigma_r}{\sigma_c}$, as shown in Table 3.

Table 3 Specimens predicting grade

NO.	σ_d	W_{et}	R	D	$\frac{\sigma_r}{\sigma_c}$	Predicting grades
3	38.37	15.53	2053	0.48	78.9%	Third
4	42.26	17.66	3258	0.56	76.48%	
2	80.72	14.61	1230	0.60	82.62%	Second
5	99.49	18.31	1480	0.65	84.21%	
8	57.02	6.72	1940	0.72	84.19%	
1	89.64	17.66	3258	0.79	87.78%	First
6	107.3	19.75	1280	0.72	86.53%	
7	103.2	18.62	1270	0.85	86 %	

Table 4 Samples degradation value L

NO.	$\frac{\sigma_r}{\sigma_c}$	Predicting grade	L
1	75%-80%	Third	0.91
4			0.77
3	80%-85%	Second	1.12
5			1.04
8			14.29
2	85%-90%	First	20
6			16.67
7			25

Table 5 Average value of each grade

Predicting grade	σ_d	W_{et}	R	D
Third	40.32	16.60	2655.5	0.52
Second	79.08	13.20	1550	0.66
First	100.05	18.68	1936	0.79

Compared with the deterioration value L

As shown in Table 4, the L value corresponded to the predicting grade. L value increased with the increase of predicting grade. It showed that the classification was reasonable. The L value differed between each grade greatly, the difference of L value was small in the same grade. However, X_8 degradation value was 14.29, which was very different from those second rocks. It might be that the internal heterogeneity of X_8 was very large, and there was weak structure surface. When the stress was up to the yield limit, the microcracks just extended through to the weak area, which was the cause of the big L value. It showed that the degradation model could be adaptable to the difference between the rocks, and made it better to classify the rocks.

$\sigma_d(x_1)$, $W_{et}(x_2)$, $R(x_3)$, $D(x_4)$ were as discriminant factors, the predicting grade was divided into the third warning grade (G_1); the second warning grade (G_2); the first warning grade (G_3). That was $G = (X_1, X_2, X_3, X_4)^T$, the main calculation process was as follows:

Calculated by Eq. (1):

$$p_1 = \frac{1}{4}, p_2 = \frac{3}{8}, p_3 = \frac{3}{8}$$

Calculated by Eq. (2), specimens mean and covariance:

$$u_1 = (40.32 \quad 16.60 \quad 2655.5 \quad 0.52)^T$$

$$u_2 = (79.08 \quad 13.20 \quad 1550.0 \quad 0.66)^T$$

$$u_3 = (100.05 \quad 18.68 \quad 1936.0 \quad 0.79)^T$$

It could be clearly shown from the specimens mean that the higher the level of predicting, the greater the damage value. In addition, the elastic energy also increased with the rise of the warning grade, it indicated that the internal energy accumulation was the source of rock failure.

The mean vector matrix of the sample is as follows:

$$\bar{X} = [u_1, u_2, u_3]$$

$$\bar{X} = \begin{bmatrix} 40.32 & 79.08 & 100.05 \\ 16.60 & 13.21 & 18.68 \\ 2655.5 & 1550 & 1936 \\ 0.52 & 0.66 & 0.79 \end{bmatrix}$$

Calculated by Eq. (3), the specimen variance matrix is obtained according to the foregoing formula:

$$S_3{}^2 = \begin{bmatrix} 7.5661 & 4.1429 & 2343.725 & 0.2556 \\ 4.1429 & 2.2685 & 1283.325 & 0.00852 \\ 2343.725 & 1283.325 & 726012 & 48.2 \\ 0.1556 & 0.0852 & 48.2 & 0.0032 \end{bmatrix}$$

$$S_2{}^2 \begin{bmatrix} 452.95 & 124.78 & -5278.45 & 0.2556 \\ 124.78 & 35.045 & -1668.05 & -0.2622 \\ -5278.45 & -1668.05 & 129700 & 21.65 \\ -0.813 & -0.262 & 21.65 & 0.00365 \end{bmatrix}$$

$$S_1{}^2 \begin{bmatrix} 85.427 & 9.093 & -10308 & -0.159 \\ 9.093 & 1.09445 & -1005.2 & -0.039 \\ -10308 & -1005.2 & 1310788 & 2.98 \\ -0.159 & -0.039 & 2.98 & 0.00425 \end{bmatrix}$$

Calculated by Eq. (4), the specimen covariance matrix and its inverse matrix are:

$$\Sigma = \begin{bmatrix} 216.85 & 54.38 & -5765.82 & -0.36 \\ 54.38 & 14.91 & -812.64 & -0.1 \\ -5765.82 & -812.64 & 721397.7 & 19.49 \\ -0.36 & -0.10 & 19.49 & 0.0038 \end{bmatrix}$$

$$\Sigma^{-1} = \begin{bmatrix} 0.207 & -0.74 & 0.001 & -5.72 \\ -0.74 & 2.75 & -0.0034 & 22.57 \\ 0.001 & -0.0035 & 0 & -0.034 \\ -5.72 & 22.57 & -0.034 & 515.132 \end{bmatrix}$$

Calculated by Eq. (5), Discriminant formulas are:

$$\omega_1(X_1, X_2, X_3, X_4) =$$
$$-4.36x_1 + 18.18x_2 - 0.019x_3 + 321.14x4 - 122.26$$

$$\omega 2(X_1, X_2, X_3, X_4) =$$
$$4.33x_1 - 12.96x_2 + 0.019x_3 + 132.85x4 - 144.63$$

$$\omega_3(X_1, X_2, X_3, X_4) =$$
$$4.24x_1 - 11.92x_2 + 0.018x_3 + 190.15x4 - 194.49$$

Table 6 Predicting results

NO.	Discriminants			Classified results	Actual grade
	W_3	W_2	W_1		
1	107.92	-76.98	-88.69	third	third
2	-0.23	181.49	183.94	first	first
3	-39.28	118.62	109.85	second	second
4	106.79	-54.22	-60.69	third	third
5	-42.54	163.34	159.33	second	second
6	-24.13	183.99	184.99	first	first
7	15.14	197.96	205.62	first	first
8	**-54.34**	**120.90**	**139**	**second**	**first**

The predicting results are shown in the following table.

The discriminant values of W_1, W_2 and W_3 were quite different, which indicated that Bayesian theory was good applicability in the predicting of rock failure. X_8 was misjudged, this exactly corresponded to the phenomenon that the L value of X_8 was larger in the second level, and the cause had been analyzed as shown in Table 5.

5. Discussion

In fact, the conventional AE parameters could be used to predict rock failure, such as AE energy count (Ganne *et al.* 2007), AE ring count (Yang *et al.* 2011; Wang *et al.* 2012) and so on. This predicting method ignored the based single on the changes of AE parameters. In addition, these parameters were related to the threshold, and there were different values in different threshold, the data could not be analyzed quantitatively. The method proposed to combine the AE parameters and other characterization parameters. In energy research, the strain energy storage index method was proposed by Wang and Park (2001), which only considered the ability of storage and release, but did not consider the internal damage. In this study, Bayesian discriminant method is used to consider the internal and external causes of rock failure, and the quantitative analysis of each parameter, the discriminant results are more reasonable and accurate.

Based on the breaking time and the damage stress threshold, this paper constructed the degradation model and quantified the degree of rock damage. In the study of multi parameter predicting (Carpinteri *et al.* 2006, Sun *et al.* 2017), there was no quantitative consideration of all factors in the comprehensive judgment, and the analysis of the degree of predicting was not carried out. In the classification of rock by the L value, the L value at the same level might be differences, which was caused by the existence of weak structure.

There were many criteria in rockburst predictability (Eberhart and Kennedy 2002, Friedman and Tukey 1974, Jian *et al.* 2014), which only predicted the intensity grade of rock burst, but ignored the time factor. Time was an essential factor in the study of rock fracture and predicting. The deterioration model L took into account the breaking time, it could predict the time of rock failure according to

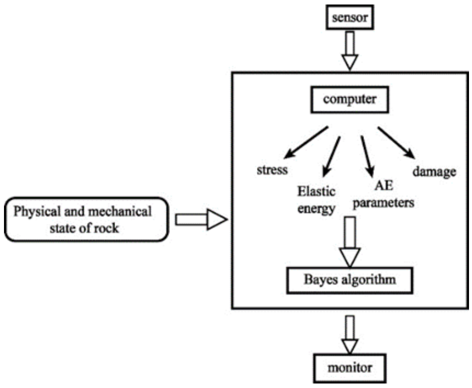

Fig. 3 Predicting grade classifier

the ratio of the damage stress threshold to the peak stress, which provided a new idea for the quantification of rock predicting.

On the basis of the above research, the idea of establishing a predicting grade classifier (as shown in Fig.3) was proposed. The sensors received the rock compression and AE data, and inputted the physi-mechanical parameters of rock to the computer. The data were analyzed by the method of mathematical statistics and analysis. The variables were extracted to analyze the variation characteristics of the parameters when rock was instability, the elastic energy, damage value and so on were used as input signals. The predicting grade was displayed on the monitor based on the Bayes discriminant calculation program.

It is an attempt to analyze precursor information through Bayesian discriminant method, and some problems are still waiting for further discussion.

(1) The selection of discriminant factors, the rock will produce a lot of physi-chemical precursor information before rock failure. We only selected four representative factors, there are more discriminant factors need further research.

(2) The sensitivity analysis of each discriminant factor, the analysis about which factor is most sensitive among the several precursors can lead to predict for different periods. The sensitivity analysis of each parameter needs new methods.

(3) The finiteness of specimens, the individual differences of specimens and the influence of sampling geology on rock failure. The physi-mechanical properties vary widely even if the same kind of rock. However, we provided an important method for predicting rock failure.

6. Conclusions

In this paper, AE parameters and the characteristics were analyzed, and the predicting point of rock failure was obtained. The deterioration model L was established, and the data integration was analyzed by the Bayesian discriminant method. The main conclusions are as follows:

• Under the loading conditions, AE impact rate exactly coincided with the change of the damage curve, and both of them correspond to the three phases of stress. The impact rate rose abruptly, and it was the same as the damage curve. The tangent at the growth point tends to positive infinity. These phenomena can be used as precursory information of rock failure.

• The degradation model L was established quantified the damage degree, it provided the precondition for classification predicting. The L value differed greatly between each grade, the difference of L value was small at the same level. The reasons for the deviation of the L value might be caused by the inhomogeneity and the weak structure.

• A multi-parameter discriminant model was established using the Bayesian discriminant method. The cracks damage threshold, AE impact rate, elastic energy and damage value were taken as input values, and it could predict rock failure classified.

Acknowledgments

We would like to thank the National Natural Science Foundation of China (No. 51574246), the National Key Research and Development Program of China (No. 2017YFC0804201), and Fundamental Research Funds for the Central Universities (No. 2011QZ01).

References

Agletdinov, E., Pomponi, E., Merson, D. and Vinogradov, A. (2016), “A novel bayesian approach to acoustic emission data analysis”, *Ultrasonics*, **72**, 89-94. https://doi.org/10.1016/j.ultras.2016.07.014.

Brady, B.T. (1969), “The nonlinear mechanical behavior of brittle rock part i—stress-strain behavior during regions i and ii”, *Int. J. Rock Mech. Min. Sci. Geomech. Abstr.*, **6**(2), 211-225. https://doi.org/ 10.1016/0148-9062(69)90036-9.

Carpinteri, A., Corrado, M. and Lacidogna, G. (2013), “Heterogeneous materials in compression: correlations between absorbed, released and acoustic emission energies”, *Eng. Fail. Anal.*, **33**, 236-250. https://doi.org/ 10.1016/j.engfailanal.2013.05.016.

Carpinteri, A., Corrado, M. and Paggi, M. (2010), “An integrated cohesive/overlapping crack model for the analysis of flexural cracking and crushing in RC beams”, *Int. J. Fract.*, **161**, 161-173. https://doi.org/ 10.1007/s10704-010-9450-4.

Carpinteri, A., Lacidogna, G. and Corrado, M. (2016), “Cracking and crackling in concrete-like materials: A dynamic energy balance”, *Eng. Fail. Anal.*, **155**, 130-144. https://doi.org/10.1016/j.engfracmech.2016.01.013.

Carpinteri, A., Lacidogna, G. and Niccolini, G. (2006), “Critical behaviour in concrete structures and damage localization by acoustic emission”, *Key Eng. Mater.*, **312**(11), 305-310. https://doi.org/ 10.4028/www.scientific.net/kem.312.305.

Cook, N.G.W. (1992), “Natural joints in rock: mechanical, hydraulic and seismic behaviour and properties under normal stress”, *Int. J. Rock Mech. Min. Sci. Geomech. Abstr.*, **29**(3), 198-223. https://doi.org/ 10.1016/0148-9062(92)93656-5.

Eberhardt, E. (1998), “Brittle rock fracture and progressive damage in uniaxial compression”, Ph.D. Dissertation, University of Saskatchewan, Saskatoon, Canada.

Frid, V. (2000), “Electromagnetic radiation method water-infusion control in rockburst-prone strata”, *J. Appl. Geophys.*, **43**(1), 5-13. https://doi.org/ 10.1016/S0926-9851(99)00029-4.

Frid, V. (2001), "Calculation of electromagnetic radiation criterion for rockburst hazard forecast in coal mines", *Pure Appl. Geophys*., **158**(5-6), 931-944. https://doi.org/ 10.1007/PL00001214.

Ganne, P., Vervoort, A. and Wevers, M. (2007), "Quantification of pre-peak brittle damage: correlation between acoustic emission and observed micro-fracturing", *Int. J. Rock Mech. Min. Sci*., **44**(5), 720-729. https://doi.org/ 10.1016/j.ijrmms.2006.11.003.

Geng, J., Sun, Q., Zhang, Y., Cao, L. and Zhang, W. (2017), "Studying the dynamic damage failure of concrete based on acoustic emission", *Constr. Build. Mater*., **149**, 9-16. https://doi.org/ 10.1016/j.conbuildmat.2017.05.054.

Ghorbani, A., Hasanzadehshooiili, H., Sadowski, L. (2018), "Neural prediction of tunnels' support pressure in elasto-plastic, strain-softening rock mass", *Appl. Sci*., **8**(5), 841. https://doi.org/10.3390/app8050841.

Goufo, E.F.D. and Kubeka, A. (2018), "Approximation result for non-autonomous and non-local rock fracture models", *Jap. J. Industr. Appl. Math*., **35**(1), 217-233. https://doi.org/ 10.1007/s13160-017-0287-3.

Hill, F.G., Cook, N.G.W., Hoek, E., Pretoriu, J.P., Ortlepp, W. and Salamon, M. (1966), "Rock mechanics applied to study of rockbursts", *J. S. Afr. Inst. Min*., **35**(1), 435-528.

Kang, Y., Ni, P., Fu, C. and Zhang, P. (2017), "Estimation of damage location of rock based on denoised acoustic emission signals using wavelet packet algorithm", *Geotech. Test. J*., **40**(6), 963-977. https://doi.org/10.1520/GTJ20170029.

Konicek, P. and Waclawik, P. (2018), "Stress changes and seismicity monitoring of hard coal longwall mining in high rockburst risk areas", *Tunn. Undergr. Sp. Technol*., **81**, 237-251. https://doi.org/10.1016/j.tust.2018.07.019.

Li, N. and Jimenez, R. (2018), "A logistic regression classifier for long-term probabilistic prediction of rock burst hazard", *Nat. Hazards*, **90**(1), 197-215. https://doi.org/10.1007/s11069-017-3044-7.

Li, N., Feng, X. and Jimenez, R. (2017), "Predicting rock burst hazard with incomplete data using Bayesian networks", *Tunn. Undergr. Sp. Technol*., **61**, 61-70. https://doi.org/10.1016/j.tust.2016.09.010.

Lockner, D. (1993), "The role of acoustic emission in the study of rock fracture", *Int. J. Rock Mech. Min. Sci. Geomech. Abstr*., **30**(7), 883-899.https://doi.org/ 10.1016/0148-9062(93)90041-B.

Martin, C.D. (1993), "The strength of massive Lac du bonnet granite around underground opening", Ph.D. Dissertation, University of Manitoba, Winnipeg, Canada.

Sato, K., Isobe, T., Mori, N. and Goto, T. (1986), "9. microseismic activity associated with hydraulic mining", *Int. J. Rock Mech. Min. Sci. Geomech. Abstr*., **23**(1), 85-94. https://doi.org/ 10.1016/0148-9062(86)91669-4.

Stanchits, S., Vinciguerra, S. and Dresen, G. (2006), "Ultrasonic velocities, acoustic emission characteristics and crack damage of basalt and granite", *Pure Appl. Geophys*., **163**(5-6), 975-994. https://doi.org/ 10.1007/s00024-006-0059-5.

Sun, X., Xu, H., He, M. and Zhang, F. (2017), "Experimental investigation of the occurrence of rockburst in a rock specimen through infrared thermography and acoustic emission", *Int. J. Rock Mech. Min. Sci*., **93**, 250-259. https://doi.org/ 10.1016/j.ijrmms.2017.02.005.

Vacek, J., Vacek, J. and Chocholoušová, J. (2008), "Rock burst mechanics: insight from physical and mathematical modelling", *Acta Polytechnica*, **48**(6).

Wang, C. L., Chuai, X.S., Shi, F., Gao, A.S. and Bao, T.C. (2018), "Experimental investigation of predicting rockburst using Bayesian model", *Geomech. Eng*., **15**(6), 1153-1160. https://doi.org/10.12989/gae.2018.15.6.1153.

Wang, C., Liu, L., Elmo, D., Shi, F., Gao, A., Ni, P. and Zhang, B. (2018), "Improved energy balance theory applied to roadway support design in deep mining", *J. Geophys. Eng*., **15**(4), 1588-1601. https://doi.org/ 10.1088/1742-2140/aab3a0.

Wang, C., Wu, A., and Lu, H. (2015), "Predicting rockburst tendency based on fuzzy matter–element model", *Int. J. Rock Mech. Min. Sci*., **75**, 224-232. https://doi.org/ 10.1016/j.ijrmms.2015.02.004.

Wang, C.L. (2018), *Evolution, Monitoring and Predicting Models of Rockburst*, Springer, Singapore.

Wang, J.A. and Park, H.D. (2001), "Comprehensive prediction of rockburst based on analysis of strain energy in rocks", *Tunn. Undergr. Sp. Technol*., **16**(1), 49-57. https://doi.org/ 10.1016/S0886-7798(01)00030-X.

Wang, S., Huang, R., Ni, P., Ranjith, P.G., and Zhang, M. (2013), "Fracture behavior of intact rock using acoustic emission: experimental observation and realistic modeling", *Geotech. Test. J*., **36**(6), 903-914. https://doi.org/ 10.1520/GTJ20120086.

Wang, Y.H., Liu, Y.F. and Ma, H.T. (2012), "Changing regularity of rock damage variable and resistivity under loading condition", *Safety Sci*., **50**(4), 718-722. https://doi.org/ 10.1016/j.ssci.2011.08.046.

Wasantha, P.L.P., Ranjith, P.G. and Shao, S.S. (2014), "Energy monitoring and analysis during deformation of bedded-sandstone: use of acoustic emission", *Ultrasonics,* **54**(1), 217-226. https://doi.org/10.1016/j.ultras.2013.06.015.

Watanabe, Y., Takai, S., Arai, Y., Yoshino, N. and Hirasawa, Y. (2001), "Prediction of mechanical properties of healing fractures using acoustic emission", *J. Orthopaedic Res*., **19**(4), 548-553. https://doi.org/ 10.1016/s0736-0266(00)00042-5.

Wei, M.D., Dai, F., Xu, N.W., Liu, Y., and Zhao, T. (2017), "Fracture prediction of rocks under mode i and mode ii loading using the generalized maximum tangential strain criterion", *Eng. Fract. Mech*., S0013794417307828. https://doi.org/ 10.1016/j.engfracmech.2017.09.026.

Yang, S.Q. and Jing, H.W. (2011), "Strength failure and crack coalescence behavior of brittle sandstone samples containing a single fissure under uniaxial compression", *Int. J. Fract*., **168**(2), 227-250. https://doi.org/ 10.1007/s10704-010-9576-4.

Zhang, O., Song, J. and Nie, X. (1991), "Application of neural network models to rock mechanics and rock engineering", *Int. J. Rock Mech. Min. Sci. Geomech. Abstr*., **28**(6), 535-540. https://doi.org/ 10.1016/0148-9062(91)91130-J.

Zhang, Y., and Ni, P. (2018), "Design optimization of room and pillar mines: A case study of the Xianglushan tungsten mine", *Quart. J. Eng. Geol. Hydrogeol*., **51**(3), 352-364. https://doi.org/10.1144/qjegh2017-037.

Zhao, J., Cai, J.G., Zhao, X.B., and Li, H.B. (2008), "Dynamic model of fracture normal behaviour and application to prediction of stress wave attenuation across fractures", *Rock Mech. Rock Eng*., **41**(5), 671-693. https://doi.org/ 10.1007/s00603-006-0127-2.

Zhu, Y H., Liu, X R., Zhou, J P. (2008), "Rockburst prediction analysis based on v-SVR algorithm", *J. China Coal Soc*., (03), 277-281. https://doi.org/10.13225/j.cnki.jccs.2008.03.025.

CC